The Effect of Cell Size on the Physical Properties of Crosslinked Closed Cell Polyethylene Foams Produced by a High Pressure Nitrogen Solution Process

M.A. Rodríguez-Pérez[1,*], J.I. González-Peña[1], N. Witten[2], J.A. de Saja[1]

[1.]Polymeric Foams Group
Condensed Matter Physics Department
University of Valladolid
47011, Valladolid, Spain
email: marrod@fmc.uva.es

[2.]Technical Department
Zotefoams Plc.
Croydon, UK

Received: 11 February 2002 Accepted: 18 June 2002

ABSTRACT

The thermal conductivity, thermal expansion, mechanical properties at low strain rates and dynamic mechanical properties of a collection of crosslinked closed cell polyethylene foams manufactured by a high pressure nitrogen solution process have been studied as a function of the cell size. The main mechanisms that influence each property and the foam microstructure have been considered to rationalise the results. A theoretical model has been used to examine the thermal conductivity values. The results have shown the extent to which reducing the cell size could improve the insulating capabilities of these materials. The effect of cell size on the mechanical properties at low strain rates is very small, as a consequence the thermal expansion does not depend on cell size. Nevertheless, the structural characteristics are seen to influence dynamic mechanical response at temperatures below 15ºC.

1. INTRODUCTION

There continues to be an interest within the scientific community in investigations relating the bulk foam properties and the foam cellular morphology. This is despite the fact that there is much confusion regarding the interpretation of the data from such investigations[(1)]. The resulting data

* To whom all correspondence should be addressed

are frequently questioned because of several experimental difficulties. For example, for some of the present technologies (especially for polyolefins) it is not a simple task to produce foams from the same base polymer with different cellular structures, moreover there is a possible influence of cellular structure on polymer morphology, in addition different authors use diverse methods to describe the cellular structure, etc.

Although it is feasible to assume that cell morphology features are associated with almost all foam properties, it is not sensible to believe that they all exert an independent and measurable influence on the foam behaviour. It is instructional to consider why one could not observe a correlation between cellular morphology and foam physical properties, a failure to establish any correlation may have resulted from an inappropriate selection of the parameters. For instance a lack of correlation can be explained by a non-representative sampling of the materials, which serves to emphasize the inherent variability frequently found in a bulk foam sample, another source could be a poor selection of the materials under study; non-homogeneous materials, materials with varying cell shape when the density is changed, materials produced from different polymer grades, etc.

Irrespective of the final application one must understand the fundamental behaviour of the cellular structure. It is clear that the knowledge of how the cell size influences the final properties of the foam is an important step towards tailoring material properties essential for advanced product design. For this reason the subject has been considered much in the past. These investigations have shown that the cell size mainly influence the thermal conductivity, the effect on the mechanical properties being negligible[2-7].

The commercial high-pressure nitrogen solution process is a versatile means of producing low-density polyolefin foams of high quality. The foams produced are excellent materials for scientific studies[8,9] due to several interesting features such as: a complete lack of residues of solid foaming agent on the final foam, an almost isotropic cellular structure and a similar cell shape for different densities. Moreover, this process technology allows foams to be produced with the same density but with a varying cell size. As has already been mentioned, it is not easy, in the majority of commercial processes, to produce polyolefin foams in which the chemical composition and density are maintained constant whilst cell size is variable over a wide range. The materials under study in this work

could help in checking and extending the previous theories because of their consistent structure and formulation.

Black foams, with a low carbon black content (below 3% approximately) are usually produced to modify the natural white colour of LDPE foams. However, as with any filler added to a given polymer system, a modification of the main physical properties of the foams should be expected. Moreover, carbon black could act as a nucleating agent for LDPE, modifying the rate of crystallisation and the size and shape of the supermolecular units forming the polymeric matrix. The extent of this modification should be considered and taken into account in the applications of these materials. In this work we have briefly considered these effects.

This work is a portion of a larger study to understand the basic relationships between the microstructure and the thermal and mechanical properties of polyolefin foams. Several physical properties (mechanical properties at low strain rates, dynamic mechanical properties, thermal expansion and thermal conductivity) of foams made of low density polyethylene (LDPE) with different cell sizes and densities have been characterised and their properties analysed in terms of the cell size and microstructure.

2. MATERIALS

The products code, nominal density (ρ), thickness, cell size description and colour of the commercial materials under study are summarised in Table 1. The foams were produced from low-density polyethylene containing a low level of carbon black (between 1.5 and 2%). The main characteristics of a solid sheet of these materials are also collected in the same table. Three foams of nominal density 45 kg/m^3 and two materials of nominal density 24 kg/m^3 were studied. The main difference between the foams with the same nominal density was the cell size. Apart from a standard material two more foams with finer and larger cells were characterised for the LD45 grade. The properties of the standard foam were compared with those of a foam with larger cells for the LD24 grade. One other LDPE foam (LD24W) of similar density to that of the LD24 foams but without the addition of carbon black was included in the study to examine the influence of the carbon black content on the physical properties of these materials.

Table 1 Main characteristics of the materials under study				
Material	Nominal density (kg/m^3)	Thickness (mm)	Type of cell	Colour
LD45FC	45	11.48	fine	Black
LD45	45	11.91	standard	Black
LD45IC	45	11.37	large	Black
LD24	24	11.49	fine	Black
LD24LC	24	10.63	large	Black
LD24W	24	10.20	standard	White
LDPE sheet	910	10.05	-	Black

These foamed samples are all cross-linked closed cell polyethylene foams manufactured by a high-pressure nitrogen gas solution process and have been kindly provided by ZoteFoams PLC (Croydon, U.K.). In this proprietary process, a polyolefin is compounded with a peroxide curing agent and extruded as a thick sheet which is then passed through an oven to effect crosslinking (gel content was approximately 40%). Slabs cut from the extruded sheet are subsequently placed in an autoclave where they are subjected to a high pressure nitrogen gas environment at temperatures above the polymer softening point. Under these conditions, the nitrogen dissolves in the polymer matrix. Upon release of the pressure, the cellular structure is nucleated and the sheet is subsequently expanded. By altering the saturation gas pressure, the amount of gas dissolved in the polymer and thus, the final foam density can be controlled and varied over a wide range. Cell size can also be controlled by changing the industrial process parameters.

3. EXPERIMENTAL

3.1 Density

Density measurements were performed by Archimedes principle using the density determination kit for the AT261 Mettler balance.

3.2 Thermogravimetric Analysis (TGA)

Thermogravimetric experiments were carried out in the temperature range between 50°C and 900°C at a scanning rate of 20°C/min. A

nitrogen atmosphere was used below 650°C; above this temperature an air atmosphere was employed. Polyethylene is flashed off between 400°C and 600°C under nitrogen, the carbon black burns off after the gas is switched to air at 650°°C. The mass of the samples was 2 mg for the 24 kg/m^3 foams and 5 mg for the 45 kg/m^3 foams. The carbon black content was then calculated by using the following equation.

$$\%\text{Carbon black} = \frac{m_2 - m_3}{m_1} 100 \qquad (1)$$

Where m_1 is the sample mass at 50°C, m_2 is the sample mass at 560°C (the LDPE has been flashed off at this temperature) and m_3 is the sample mass at 900°C (the carbon black has been burned off at this temperature). Three experiments were performed for each material, the 95% confidence error was approximately ±5% of the average value.

3.3 Scanning Electron Microscopy (SEM)

Quantitative image analysis was used to assess the type of cellular structure and apparent mean cell diameter. For this purpose, cross-sections of the foams were cut at low temperature to provide a smooth surface which, after vacuum coating with gold, were examined by SEM using a JEOL JSM-820 microscope. Each micrograph was analysed by obtaining data from 10 reference lines. Apparent cell diameter was determined by calculating the number of cells that intersected each reference line and by dividing the appropriate reference line length by the number of cells. The cell diameter was measured in the three main directions of each foam, the mean value of these three cell diameters was taken as the mean cell size of the foam.

A total of three micrographs (400 cells approximately) were randomly taken over each specimen and subjected to cell size analysis. The 95% confidence error of these three measurements was approximately ±6% of the average value for the mean cell size.

The results obtained by using the previous method were multiplied by 1.62 to take into account the relationship between the average measured length of the randomly truncated cells and the real diameter of the cell (Φ)[10].

It has been previously shown that foams produced by this high-pressure nitrogen solution process are isotropic materials[8,9], therefore it was not necessary to characterise the degree of anisotropy.

In order to obtain a more complete characterisation of the cellular structure two additional parameters were determined: the mean cell wall thickness (δ) and the mass fraction in the struts (f_s).

The thickness of thirty cell walls, randomly chosen along the foam, were measured directly in the microscope screen. The average value of these measurements was considered as the mean cell wall thickness of the foams. The 95% confidence interval of these measurements was approximately ± 8% of the average value.

Finally, the fraction of mass in the struts was obtained by means of the method proposed by Kuhn[11], measuring through four micrographs taken randomly over each specimen. The 95% confidence error of these measurements was ± 8% of the average value.

3.4 Differential Scanning Calorimetry (DSC)

Thermal properties were studied by means of a Mettler DSC30 differential scanning calorimeter, previously calibrated with indium. The weights of the samples were approximately 1.74±0.02 mg.

A first heating cycle between -40°C and 200°C at 10°C/min was performed. This experiment was used to study some characteristic properties of the polymer that comprises the cell walls of the original foams.

The crystallisation behaviour was evaluated by heating the polymer sample in the DSC pan at 200°C for 5 minutes to allow all crystallites to melt, and then cooling at a rate of 20°C/min from 200°C to -40°C. The sample was kept at -40°C for 3 minutes and then the melting behaviour was recorded by means of a further cycle, heating the sample to 200°C at a rate of 10°C/min (2^{nd} heating).

From each heating cycle two characteristics properties of the base polymer were obtained: the melting point (T_m) and the degree of crystallinity (X_c). The melting point was taken as the minimum of the melt peak in the enthalpy curve. The degree of crystallinity was calculated from the DSC curve by dividing the measured heat of fusion by the heat of fusion of a 100% crystalline material (288 J/g for low density polyethylene)[12]. A linear correction factor was also included to take into account the carbon black content in the foams. From the cooling cycle the crystallisation temperature (T_c), obtained as the maximum in the enthalpy, and the degree of crystallinity were also measured.

To study the possible differences between the crystallisation of the different foams non isothermal crystallisation experiments were carried out. Before each cooling, the samples were heated at 200°C for 4 min in order to erase any previous thermal history. The measurements were performed from 200°C to –40°C at the following cooling rates: 1, 2, 5, 10 and 20°C/min.

The non-isothermal crystallisation processes were studied following the method develop by Dobreva and Gutzow[13] for the study of the crystallisation kinetics of molten polymers in the presence of nucleating agents. The relationship proposed by these authors is the following:

$$\log q = \text{const.} - \frac{B}{2.3\Delta T^2} \qquad (2)$$

Where q is the rate of crystallisation, ΔT is equal to $T_m - T_p$, with T_m the melting temperature and T_p the crystallisation temperature of the samples.

The possible differences between the crystallisation process in the foams can be evaluated by using the following parameter:

$$\varphi = \frac{B^*}{B^0} \qquad (3)$$

Where B^0 is the value of B for the solid material and B^* is the value of B for the foamed materials.

From the experimental slopes in the representation log q versus $1/\Delta T^2$, according to equation 2, it is possible to obtain the B values. Finally, by using equation 3, the parameter φ can be estimated.

3.5 Etching

The foams were chemically treated, to reveal the crystalline morphology. The permanganate etching method involved the following steps[14].

1. Addition of 7% potassium permanganate to concentrated sulphuric acid.

2. Treatment of the specimen for 60 min at 0°C.

3. Etching stopped, washing of the sample in dilute sulphuric acid at

0°C and leaving to decant for 10 min, then washing successively with hydrogen peroxide, water and acetone.

After the treatment the samples were vacuum coated with gold and examined by SEM.

3.6 Thermal Conductivity

A Rapid K Heat Flow Meter from Holometrix was used for the thermal measurements. Heat flow through the test sample, (q), results from having a temperature gradient, (ΔT), across the material. The thermal conductivity λ is defined according to Fourier's equation:

$$q = \lambda A \frac{\Delta T}{d} \qquad (4)$$

where A is the cross-sectional area of the sample and d is the sample thickness.

The heat flow meter is a thermopile which gives an output of 40 μV for a temperature drop of 1°C. It is a 10 cm side square which occupies the central portion of the cold face of the equipment. The total face area is a square of 30 cm side, the remaining portion acts as a shield that keeps the heat flow uniform in the central measurement section. The method is not absolute, and therefore needs to be calibrated using a standard sample. Once this has been done, the heat flow per unit area can be found from the reading of the heat flow transducer, and the thermal conductivity of the sample can thus be calculated using equation 4.

The measurements were made under steady state heat flow conditions through the test sample. These were done in accordance with ASTM C518 and ISO DIS 8301 methods. Square samples of 30 cm side were used for all experiments. A dispersion of less than 1% in two consecutive readings was taken as a criterion to ensure that the measurements were done under steady state conditions. The time lap between readings was 10 minutes. The measurements were performed at 24, 30, 40 and 50°C. Each experiment was repeated 5 times in order to obtain an average value. The precision of the apparatus was approximately 5%.

3.7 Compression Experiments at Low Strain Rates

Compressive stress (σ) strain (ε) curves were measured using an Instron machine (model 5500R6025) at room temperature and at a strain rate

of 0.1 s^{-1}. The maximum static strain was approximately 75% for all the experiments.

Following this first loading cycle, the stress strain behaviour at a rate of 0.1 s^{-1} was also recorded during unloading (recovery behaviour). This load and recovery cycle was repeated 5 times on each of the samples (5 cycles applied consecutively). The 5 cycles were then used to study the influence of the mechanical history on the properties of each foam. The diameter of the test samples was 10 centimetres and three samples were tested for each type of material under study in order to obtain the average response.

The following mechanical properties were obtained from the previous experiments.

1) The slope of the initial zone of the stress strain curve for each cycle E^i. For the first cycle this slope can be considered as the elastic modulus of the foam, E.

2) The non-recoverable strain for each cycle nr^i

$$nr^i = \frac{\varepsilon_0^i}{\varepsilon_m^{(i-1)}} 100 (i > 1, nr^1 = 0) \quad (5)$$

where $\varepsilon_m^{(i-1)}$ is the maximum strain in the cycle number (i-1), and ε_0^i is the minimum strain in the cycle number i.

3) The collapse stress and effective pressure of the gas were also computed for the first cycle (see below).

The 95% confidence interval was approximately ±5% for the different properties.

3.8 Thermal Expansion

The linear thermal expansion coefficient (α) can be determined by:

$$\alpha = \frac{1}{l_0} \frac{dl}{dT} \quad (6)$$

where l_0 is the original length at a reference temperature (25°C in this work) and l is the length of the sample at a temperature T.

The thermomechanical experiments were conducted on Perkin-Elmer TMA7 test equipment. The applied stress was 130 Pa, sufficient to ensure that the probe remained in contact with the sample and small enough to allow the compressive strain to be neglected. These tests were carried out with the same geometric arrangement as that used in the dynamic mechanical experiments.

To obtain the thermal expansion coefficient outside of the temperature range where thermal transitions were present[15], experiments were performed as follows:

The foam was cooled from room temperature to 5°C, and was kept at this temperature for 15 minutes. The heating cycle was then carried out from 5°C to 25°C at 1°C/min. The foam sample was then maintained at 25°C for 15 minutes. Each of the materials were scanned three times. The standard deviation of the three measurements was approximately ± 4% of the mean value.

3.9 Dynamic Mechanical Analysis (DMA)

The storage modulus (E'), loss modulus (E''), and loss tangent or loss factor (tan δ) were obtained in a parallel plate measurement system. The properties were measured at frequency of 1 Hz, over a temperature range of -60°C and 100°C and with a heating rate of 5°C /min. The applied static strain and dynamic strain were chosen in the low strains range (2% static strain and 0.10% dynamic strain), where the mechanisms that control the sample's behaviour are known to be the cell edges bending and the cell faces stretching[16,17]. The plate diameter was 15 mm and the test specimens were prepared in a cylindrical shape with the same diameter. Three experiments were carried out for each material. The 95% confidence interval was approximately ±6% for the modulus results and ±4% for the loss factor.

4. RESULTS

4.1 Microstructure

Cellular Structure

The density and carbon black content are summarised in Table 2. As expected, the densities are very close to the nominal values and the carbon black content ranges between 1.6 and 2.0%. Moreover, the

Table 2 Density (ρ) and black carbon content in the foams		
Foam	ρ(kg/m^3)	Black carbon content (%)
LD24	23.6	1.9
LD24LC	23.7	1.6
LD45FC	42.6	1.6
LD45	42.3	1.7
LD45IC	41.3	2.0
LDPE	910	1.9
LD24W	24.6	0.0

differences in carbon black content between foams with the same nominal density are insignificant.

Two typical images of the closed cell structure of the foams under study can be observed in Figure 1. The cellular structure of the foams is isotropic and no residues of foaming agent can be perceived. The main characteristics

Figure 1 Micrographs of the foams a) LD24, b)LD24LC

(a)

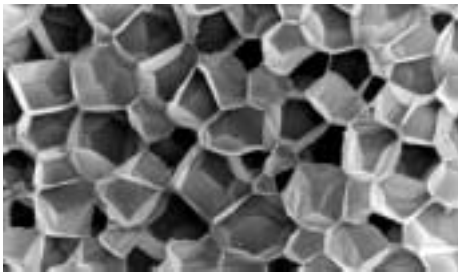

(b)

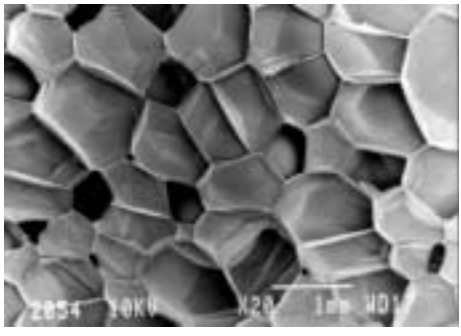

of the cellular structure are given in Table 3. As can be observed, a wide range of cell sizes and mean cell wall thicknesses were measured, i.e. cell size ranges between 315 and 950 μm for the LD24 grade and between 350 and 825 μm for the LD45 grade. The mean cell wall thickness covers the range between 1.7 and 7 μm. Finally, the mass fraction in the struts is found to be non-negligible for the black materials and ranges between 0.30 and 0.45. It is well known that for a given cell shape, it is possible to determine the mean cell wall thickness (δ) by using the equation:

$$\Phi(1 - f_s)\frac{\rho}{\rho_0} = C\delta \qquad (7)$$

where Φ is the cell size, f_s is the mass fraction in the struts, ρ is the foam density, ρ_0 is the density of the base polymer, δ is the mean cell wall thickness and C is a constant which depends on the cell shape. It can be shown that C has values of 3.46 for a pentagonal dodecahedron cell shape[4] and 3.35 for tetrakaidecahedral cell architecture[18]. The experimental data for the foams under study fits equation (7) with a C value of 3.57 (Figure 2). This result seems to indicate that all the materials under study have similar cell shapes, comparable to that found in other studies for white low-density polyethylene and ethylene vinyl acetate foams produced from the same process[2,3] .

Polymer Morphology

The melting temperature, degree of crystallinity and crystallisation temperature are collected in Table 4. The melting point and crystallisation

Table 3 Main structural characteristics of the studied foams. ϕ is the means cell size, δ is the mean cell wall thickness and f_s is the fraction of mass in the struts

Foams	ϕ(μm)	δ(μm)	f_s
LD24	315	1.6	0.45
LD24LC	956	5.5	0.41
LD45FC	353	3.2	0.40
LD45	438	4.0	0.30
LD45IC	825	7.0	0.32
LD24W	312	1.9	0.16

Figure 2 Linear fit of the experimental data to the equation 7

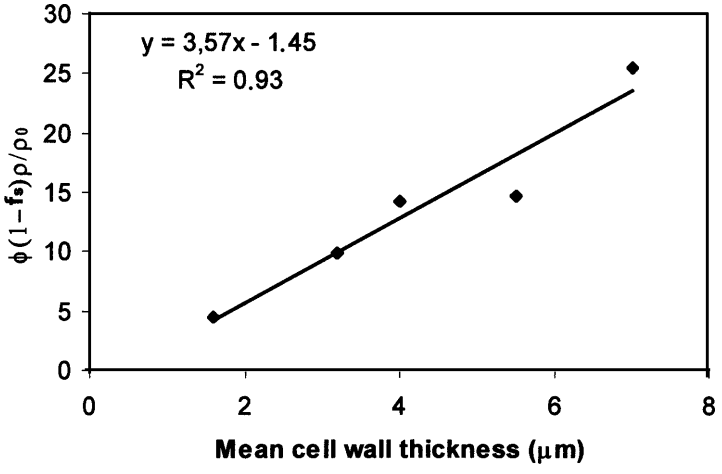

Table 4 Melting point and crystallinity of the foams. χ_1 and T_{m1} are the crystallinity and melting point measured in the first heating segment, χ_c and T_c are the crystallinity and crsytallisation temperature measured in the cooling segment, χ_2 and T_{m2} are the crystallinity and melting point measured in the second heating segment

Foam	χ_1	T_{m1}	χ_c	T_c	χ_2	T_{m2}
LD24	43.82	110.18	42.88	95.74	44.54	110.36
LD24LC	43.39	111.05	43.28	95.55	41.56	110.88
LD45FC	42.8	110.85	42.7	95.27	42.24	111.19
LD45	42.96	111.00	44.46	95.25	42.64	111.17
LD45LC	43.48	111.86	42.73	94.07	43.86	112.03
LD24W	43.8	108.60	39.5	92.4	38.8	109.6
LDPE	44.35	108.15	45.29	93.77	45.29	108.49

temperature are typical for materials based on LDPE; melting point in the second heating is approximately 111°C and degree of crystallinity lies between 41 and 45% for the black foams. The differences between the black foams are small and within the experimental error, which suggests that the same LDPE grade was employed to produce all the foams. The

white LD24 foam has a lower degree of crystallinity and melting point (2nd heating) which may indicate that a different LDPE grade was used to produce this material, another possibility to explain this result would be connected to a possible effect of the carbon black on the foams crystallisation.

Figure 3 shows a typical high magnification micrograph of the front view (light beam normal to the wall) of an etched cell wall in which supermolecular units can be observed. These structures are similar to those observed in white low-density polyethylene foams produced from the same process and with similar densities[19].

It has previously been established that the supermolecular units for white low-density PE foams are formed from radiating fibrils, i.e., groups of lamellar crystals including amorphous inter-layers. The fibrils initiate at nuclei on the cell wall surface and branch as they grow radially away from the nucleus. The growth direction of the fibrils changes; originally it grows in the plane of the cell wall at the cell/gas surface, but later it grows almost perpendicular to the surface as it reaches the mid-plane of the cell wall. The supermolecular units meet others growing from the other side of the cell wall face, and terminate their growth. The final shape is almost hemispherical on the initial face. In white low-density PE foams, the diameter of the supermolecular units in the plane of the cell wall increases linearly with the thickness of the cell wall (Figure 4). This trend is not observed for the black foams under study here however (Figure 4). In fact, the diameter of the supermolecular units seems to be almost constant as a function of the cell wall thickness. This interesting difference between white and black foams produced from the same process technology and

Figure 3 Micrographs of a cell wall after etching (electron beam perpendicular to the wall surface) LD24 foam

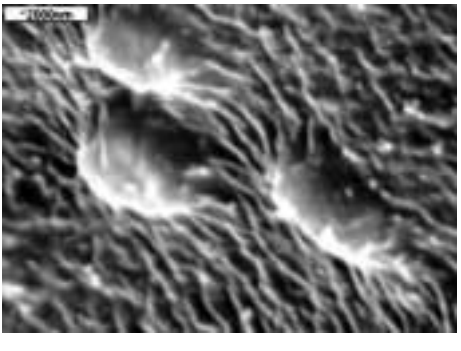

Figure 4 Supermolecular units diameter as a function of the cell wall thickness

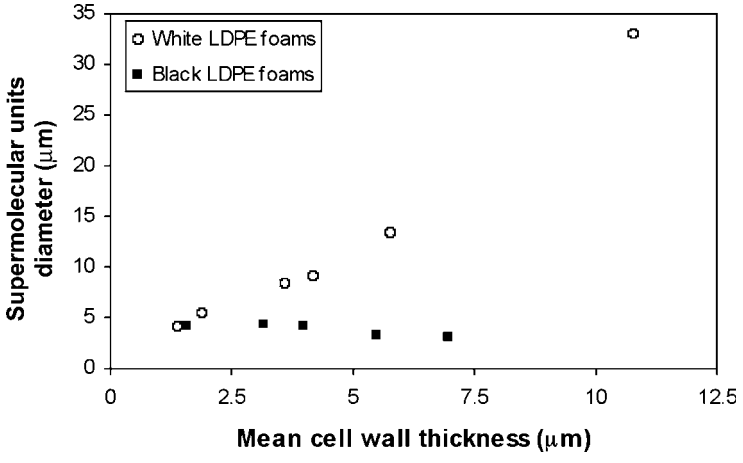

materials would seem to be connected to a possible nucleating effect of the carbon black on the foam crystallisation.

The values of the parameter φ are collected in Table 5, as can be observed the crystallisation in the foams differs considerably to that of the solid sheet. Moreover, the values of this parameter are higher for the high density foams, and for a given density seems to be higher for the foams with larger cell sizes. The white foam shows the fastest rate of crystallisation.

Table 5 Values of the parameter φ	
Foams	φ
LDPE	1
LD24	1.12
LD24LC	1.18
LD45FC	1.48
LD45	1.34
LD45LC	1.85
LD24W	0.94

It is useful to summarise the results of the structural characterisation before considering the macroscopic properties. The foams under study were produced from a similar initial formulation, which means a similar LDPE grade and carbon black content. Moreover, for each foam grade LD45 and LD24, the density was almost constant. Therefore, the change in properties has to be explained in terms of differences in cellular structure and/or differences in the matrix polymer morphology. On the one hand, the study of theses cellular structures has shown that the high-pressure nitrogen solution process technology yields foams with similar cell shapes but different cell sizes, and as a consequence different cell wall thickness. On the other hand, the analysis of the matrix polymer morphology has detected the supermolecular units for these materials, similar in shape to that found for white LDPE foams, but smaller in size. Moreover, the degree of crystallinity and melting point was similar for all the black foams under study. The examination of the crystallisation kinetics has revealed a different crystallisation rate for each material, and shows differences to that of a solid sheet of similar composition. The rate of crystallisation is lower for the 45 kg/m^3 density foams and appears to decrease as the cell size increases. Therefore, it is feasible to believe that a slightly different polymer morphology would be present in foams with different densities and/or cell sizes.

In summary then, it can be concluded that the selected materials are suitable for the purpose of this study, the variation of the properties has to be understood in terms of different cell size and/or cell wall thickness and in terms of small differences in the matrix polymer morphology which could have its source in the dependence between the crystallisation kinetics and the cellular structure. Therefore, in the analysis of the macroscopic properties it will not be easy to separate the possible effects of cell size and polymer morphology due to the inherent relationship between these two characteristics.

4.2 Thermal Conductivity

The thermal conductivity as a function of the temperature is shown in Figure 5. The thermal conductivity increases linearly with temperature for all of the materials studied. The linear fit parameters are summarised in Table 6. The slope of the curve increases with cell size and for similar cell sizes the slope is steeper for the foams with lower density. These slopes are lower than those found for white LDPE foams[20].

Figure 5 Thermal conductivity as a function of temperature

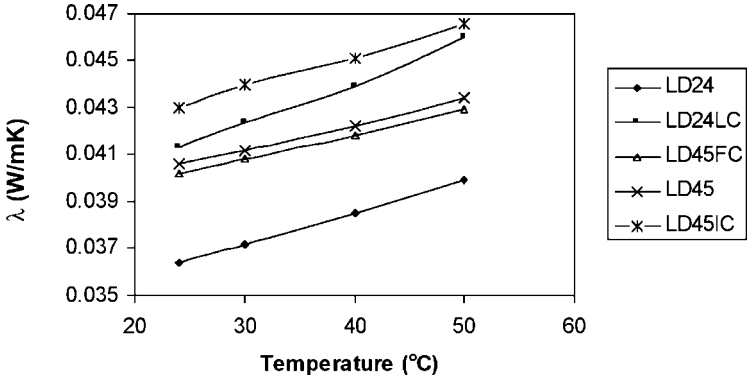

Table 6 Linear fit parameters for the experimental thermal conductivity versus temperature			
Foam: λ=AT+B	A (W/mK^2)	B (W/mK)	r^2
LD24	1.34 10^{-4}	3.32 10^{-2}	0.999
LD24LC	1.78 10^{-4}	3.70 10^{-2}	0.995
LD45FC	1.04 10^{-4}	3.77 10^{-2}	0.999
LD45	1.07 10^{-4}	3.80 10^{-2}	0.998
LD45LC	1.35 10^{-4}	3.98 10^{-2}	0.995

The behaviour as a function of cell size can be seen in Figure 6a and 6b. A linear increase of the thermal conductivity with cell size is observed for the LD45 grade. The thermal conductivity increases by 4.6% as the cell size changes from 353 μm to 825 μm (57% increase) for the LD45 foams, and by 11.9% as the cell size changes from 315 μm to 956 μm (67% increase) for the LD24 foams.

The thermal conductivity value at room temperature for the black LD24 foam is lower that that shown by the white LDPE foam (LD24W). The

Figure 6 Thermal conductivity as a function of cell size. a) LD45 grade, b) LD24 grade

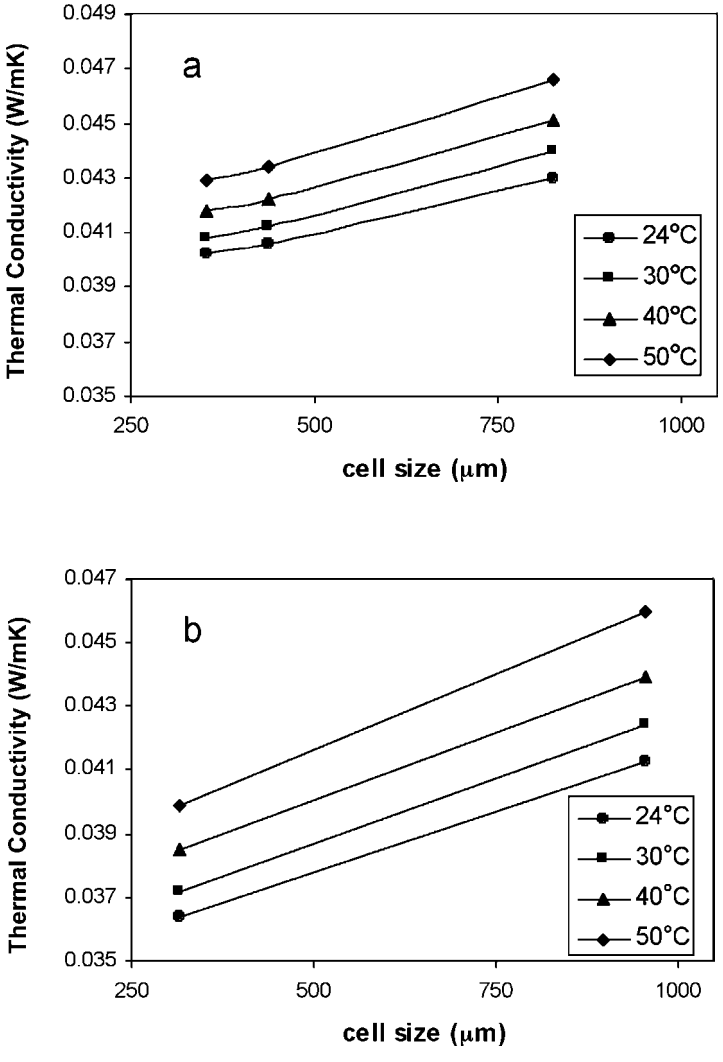

thermal conductivity of this material at 24°C is 0.0372W/mK, 2% higher than that of the LD24 black foam.

Previous works[3,20] have shown that the following equation is able to predict with good precision the thermal conductivity of low-density polyethylene foams produced by a high-pressure nitrogen process or indeed a compression moulding process.

$$\lambda = \lambda_{gas} V_{gas} + \left(\frac{2}{3} - \frac{f_s}{3}\right)\lambda_{poly} V_{poly} + \frac{4\sigma T^3 L}{1 + \left(\frac{L}{\Phi}\right)\left(\frac{1}{T_N} - 1\right)} \qquad (8)$$

In this equation, all the parameters can be measured or estimated. On the one hand, λ_{gas} is the thermal conductivity of the gas which fills the cells, λ_{poly} is the thermal conductivity of the matrix polymer, V_{gas} is the volume fraction of gas and V_{poly} is the volume fraction of polymer, f_s is the mass fraction in the struts. On the other hand, σ is the Stefan-Boltzman constant, T is the temperature, L is the foam thickness, Φ is the mean cell size and T_N is the net fraction of radiant energy sent forward by a solid membrane of thickness L_s (this quantity can be represented in our work by the mean cell wall thickness) . T_N is given by the equation:

$$T_N = \frac{(1-r)}{(1-rt)}\left\{\frac{(1-r)t}{(1+rt)} + \frac{(1-t)}{2}\right\} \qquad (9)$$

where r is the fraction of incident energy reflected by each gas-solid interface. This quantity is related to the refractive index of the plastic ω by:

$$r = \left\{\frac{\omega - 1}{\omega + 1}\right\}^2 \qquad (10)$$

and the coefficient t is the fraction of energy transmitted through the solid membrane (thickness L_s), which is given by the Bouguer's law:

$$t = \exp(-aL_s) \qquad (11)$$

where a is the absorption coefficient of the plastic.

The first term in equation 8 is the contribution to the thermal conductivity from the gas, and depends on its own nature. In our case, the gas is air at atmospheric pressure for which the conductivity at 24, 30, 40 and 50°C has been taken as 0.0257, 0.0262, 0.0269 and 0.0277[21]. The gas in the cells is air, since gases such as nitrogen and air can diffuse in and out of LDPE foams and achieve equilibrium on a time scale of weeks[22].

The second term in equation 3 is associated with the contribution of the solid phase. Therefore, as a first approximation, it is reasonable to use

the measured value of the thermal conductivity of the solid sheet to estimate (λ_{poly}) in the former equation. The values were 0.231, 0.233, 0.236 and 0.239 W/mK at 24, 30, 40 and 50ºC respectively.

The third term in the equation accounts for the heat flow due to radiation. To compute this contribution the refractive index and the absorption coefficient has to be estimated. Values obtained for white LDPE foams (ω = 1.51 and a = 661 cm^{-1}) were initially tried[19].

The differences between the theoretical and experimental values are collected in Table 7.The predictions are in reasonably good agreement with the experiments for the foams of 45 kg/m^3 nominal density, however larger differences are observed for the 24 kg/m^3 density foams. Carbon black should increase the absorption coefficient and refractive index of the base polymer, therefore it is reasonable to use other values for the optical properties of the cell walls. In a second step, the model was applied using as values of a and ω 800 cm^{-1} and 1.55 respectively. The numerical results are given in Table 8. The predictions for the LD45 foams remain satisfactory, and those for the LD24 materials are improved. Figure 7 shows an example of the experimental and theoretical values as a function of the temperature. It is interesting to mention that the model, apart from predicting reasonable numerical values for the thermal conductivity, accounts for the linear trend of thermal conductivity with temperature. The slopes of the model curves follow the same trends as the experimental ones, however the values are overestimated (Table 9). The same equation has been used for white LDPE foams[20] showing a good agreement with the experimental results in the predictions of the slopes. A possible explanation for this behaviour could be connected to

Table 7 Differences (%) between the experimental and theoretical values of the thermal conductivity at different temperatures. a=1.51, ω=6.61 10^4 m^{-1}

Espuma	24°C	30°C	40°C	50°C
LD24	7.6	8.2	9.4	10.4
LD24LC	6.6	7.1	8.8	9.3
LD45FC	-0.8	0.2	2.0	3.6
LD45	0.6	1.7	3.5	4.9
LD45IC	0.3	0.8	2.9	4.2

Table 8 Differences (%) between the experimental and theoretical values of the thermal conductivity at different temperatures. a=1.55, $\omega=8.0\ 10^4\ m^{-1}$

Espuma	24°C	30°C	40°C	50°C
LD24	4.4	4.9	5.9	6.8
LD24LC	2.4	2.8	4.3	4.7
LD45FC	-4.1	-3.1	-1.5	0.0
LD45	-2.8	-1.8	-0.1	1.1
LD45IC	-3.6	-3.2	-1.3	-0.1

Table 9 Theoretical fits thermal conductivity vs. temperature ($a=1.55$, $a=8\ 10^4\ m^{-1}$)

Foam: $\lambda=AT+B$	A (W/mK^2)	B (W/mK)	r^2
LD24	1.82 10-4	3.64 10-2	0.999
LD24LC	2.28 10-4	3.93 10-2	0.999
LD45FC	1.63 10-4	3.71 10-2	0.999
LD45	1.69 10-4	3.78 10-2	0.999
LD45LC	1.94 10-4	3.91 10-2	0.999

Figure 7 Experimental and theoretical thermal conductivity for the LD24 foam as a function of temperature

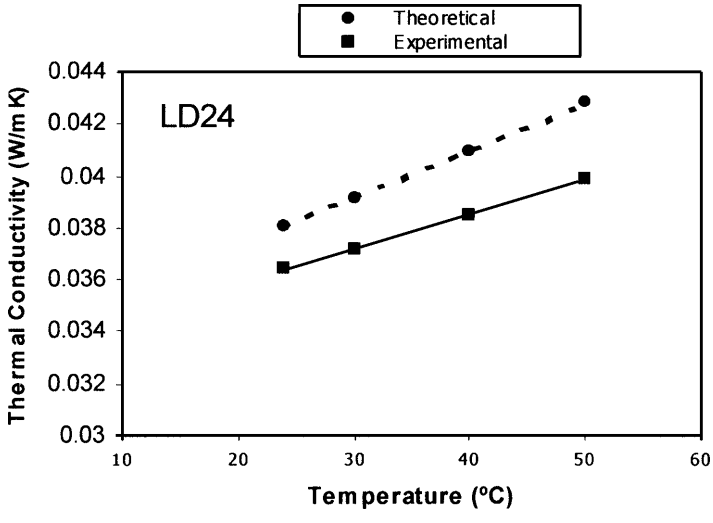

a dependency of the optical properties of the matrix polymer with temperature. The important differences between the thermal conductivity of the LD45 and LD24 foams (higher than those expected and given by equation 8) could have its origin in the different microstructure of foams of different densities.

The thermal conductivity as a function of cell size, observed in the experimental results, is explained by the model though the contribution of the radiation term. In addition, carbon black increases the conductivity through the solid phase, however it has a larger contrary effect on the radiation term, decreasing it. As a consequence black foams are slightly better thermal insulating materials.

4.3 Mechanical Properties at Low Strain Rates

The data for the slope of the initial part of the compressive stress strain curve and non-recoverable strain as a function of the cell size can be observed in Figures 8a and 8b for the LD45 grades and in Figures 9a and 9b for the LD24 grades. The properties dramatically change after the first loading/unloading cycle. This is due to plastic deformation in the cell walls that takes place during the first cycle, in which the strain reached a value of 75%.

Apart form the higher modulus of the higher density foams it is also interesting to note the differences as a function of cell size. These differences are small in the first cycle, i.e. for both grades the Young's modulus is 1.5% higher for the foams with larger cell sizes. However, in subsequent loading/unloading cycles the foams with higher larger cell sizes show a reduced Young's modulus (3% lower for the LD24 grade and 4% lower for the LD45 grade). The behaviour of the non-recoverable strain as a function of cell size is contradictory, on the one hand this property increases with cell size for the 45 kg/m^3 foams, but decreases for the 24 kg/m^3 foams.

The collapse stress and effective pressure of the gas were computed by fitting the stress (σ) strain (ε) data between 20% and 60% strain to the well-known equation[18].

$$\sigma = \sigma_c + \frac{p_a(1-2\nu)}{(1-\varepsilon-\rho/\rho_0)}\varepsilon \qquad (12)$$

Where σ_c is the collapse stress, $p_a(1-2\nu)$ is the effective pressure of the gas in the cells, p_a is the atmospheric pressure (101 kPa) and ν is the Poisson ratio. The results are given in Table 10. As can be observed the collapse stress seems to be almost constant, whilst effective pressure of the gas decreases as a function of cell size.

It has been reported elsewhere that Young's modulus and collapse stress are independent on cell size. Density, fraction of mass in the struts,

Figure 8 Mechanical properties at low strain rates for the LD45 grade as a function of cell size. a) slope of the initial part of the stress strain curve. b) non-recoverable strain

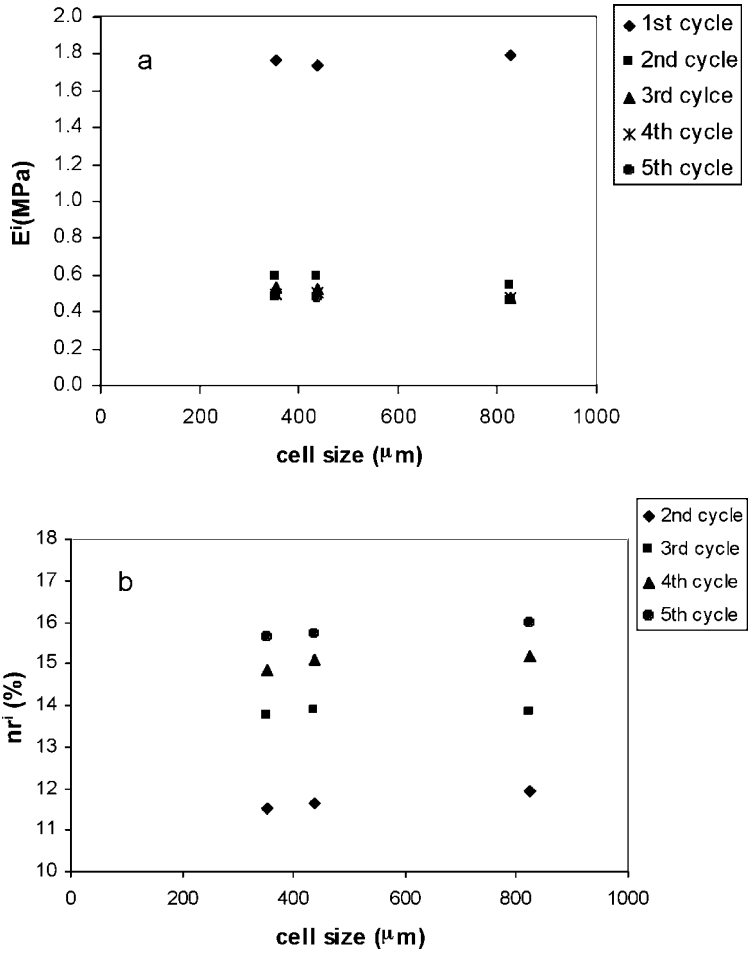

Figure 9 Mechanical properties at low strain rates for the LD24 grade as a function of cell size. a) slope of the initial part of the stress strain curve. b) non-recovered strain

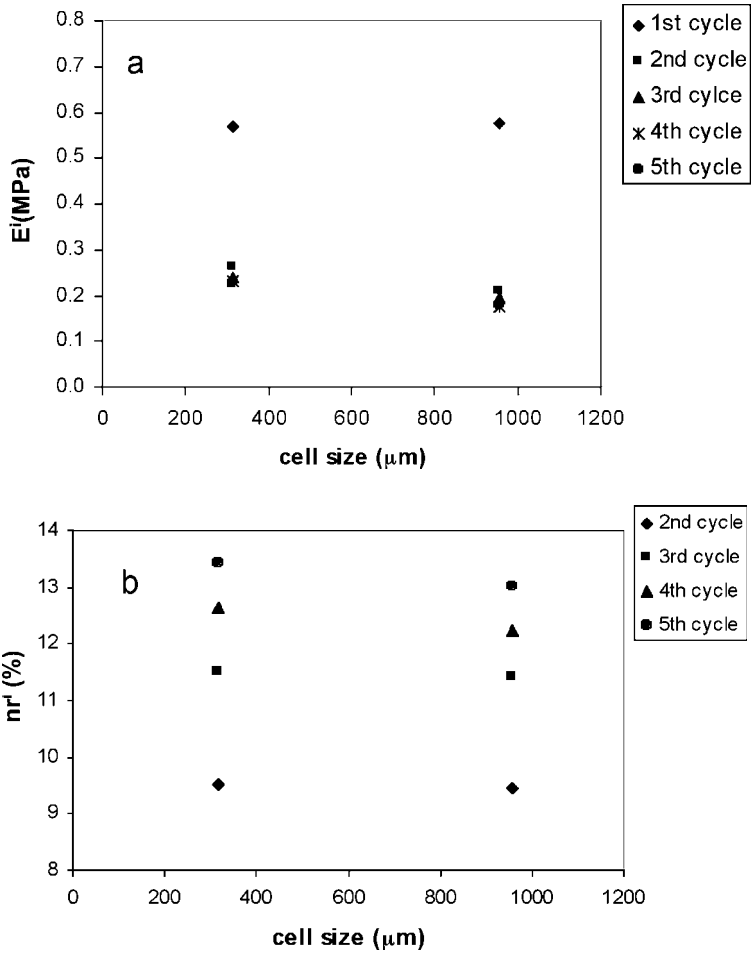

Table 10 Collapse stress and effective gas pressure for the foams under study		
Foam	σ_c (MPa)	P_a (1-2ν)
LD24	$2.57\ 10^{-2}$	72.8
LD24LC	$2.14\ 10^{-2}$	65.7
LD45FC	$6.41\ 10^{-2}$	76.8
LD45	$6.44\ 10^{-2}$	78.5
LD45LC	$6.31\ 10^{-2}$	65.5

stiffness of the cell walls and struts are noted as the most influential factors on these two properties[7,8,23]. The experimental results mainly agree with these investigations. The slightly higher modulus of the LD24LC and LD45 may be explained by a lower polymer mass fraction contained in the struts, a higher carbon black content for these two materials or a slightly different polymer morphology.

Table 11 summarises several values of the mechanical properties of the LD24 white and black foams. The carbon black improves the Young's modulus and collapse stress in the first loading cycle, however after the first cycle the slope of the initial part of the compressive stress strain curve is lower for the black foam than for the white material. Carbon black acts improving the stiffness of the cell walls and reducing its resilience. And additional effect due to the modification of the matrix polymer morphology caused by the different crystallisation process should also be expected.

Table 11 Slope of the initial part of the stress strain curve collapse stress for the LD24 white and LD24 black foams

	E^1(MPa)	E^2(MPa)	E^3(MPa)	E^4(MPa)	E^5(MPa)	σ_c(MPa)
LD24	0.567	0.262	0.239	0.231	0.228	0.026
LD24W	0.529	0.267	0.260	0.257	0.253	0.023
% difference	6.7	-1.9	-8.8	11.3	-11.0	11.5

4.3 Thermal Expansion

The linear thermal expansion coefficient between 5 and 25°C is plotted as a function of foam the cell size in Figure 10. This physical property is almost constant as a function of cell size. However, as expected the foams with lower densities produced a higher value of the expansion coefficient.

It has been previously published that the main mechanisms that influence the linear thermal expansion are the expansion of the gas inside the cells and the stiffness of the elements that form the cellular structure[15]. The lower the content and/or the stiffer the cell walls and struts are will tend to reduce the expansion. As a consequence foams of higher density, i.e. those which have stiffer cell walls and struts and a lower gas content, will show lower values of the thermal expansion coefficient. Furthermore, and taking into account that Young's modulus also depends on the

Figure 10 Thermal expansion as a function of the cell size

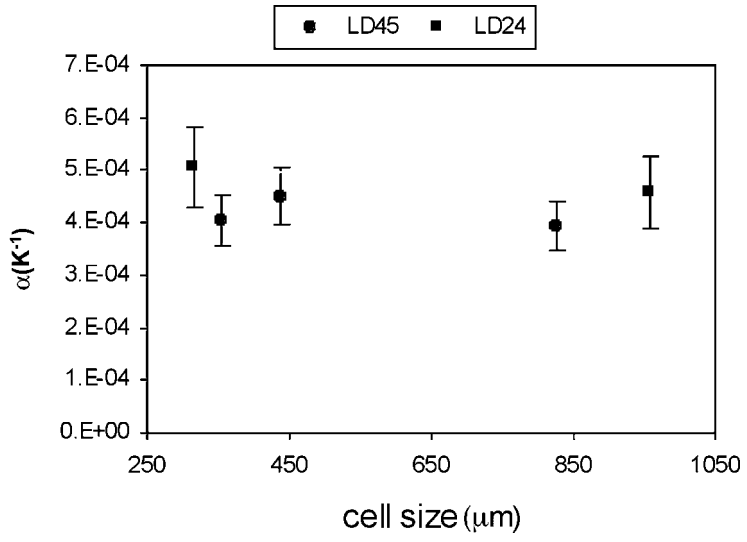

stiffness of the cell walls and struts[7], an inverse relationship should exist between the Young's modulus and the thermal expansion coefficient, a higher modulus would suggest a lower value of the expansion. The experimental results have shown this behaviour, the foams with larger cells displayed slightly higher modulus results and gave lower values of the thermal expansion coefficients.

4.4 Dynamic Mechanical Analysis

The storage modulus as a function of the temperature is presented in Figure 11a. At temperatures above 15°C foams with different cell sizes have similar modulus, however below this temperature the foams with large cell sizes, i.e. LD24LC and LD45LC, give a lower modulus than the foams with smaller cell sizes. If we focus our attention on the tan δ curve in the temperature range of the β relaxation (around -20°C), it is also possible to observe that the foams with larger cell sizes present a more intense β relaxation (Figure 11b).

The dynamic mechanical results are quite interesting because they show that under certain conditions the mechanical response of foams may depend on cell size. At temperatures below room temperature, in the zone

Figure 11 Dynamic mechanical properties of the foams under study. a) Storage modulus, b) Loss factor

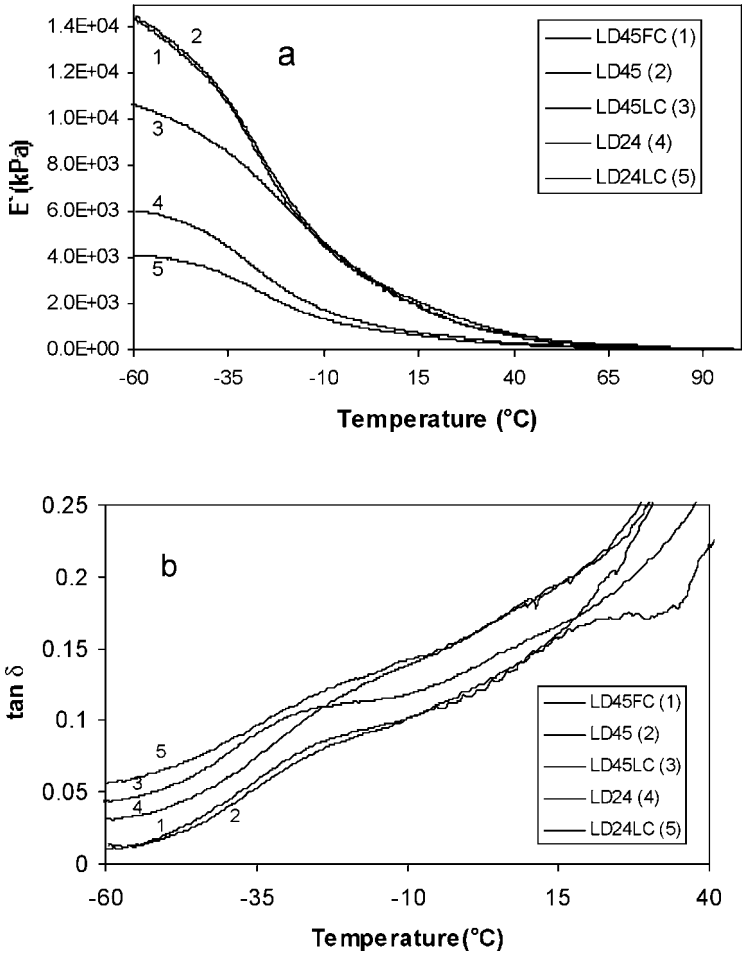

of the β relaxation the storage modulus and loss tangent show a dependence on cell size. The explanation for this result could be associated to the different crystallisation kinetics of foams of different cellular structure. It is known[24,25] that the behaviour of solid LDPE in the β relaxation zone is sensitive to the morphology of the polymer at the interface between the crystalline and amorphous regions. A different rate of crystallisation could modify the polymer morphology and as a consequence the dynamic mechanical response in this temperature range.

CONCLUSIONS AND OUTLOOK

The polyolefin foams produced by the high-pressure nitrogen solution process technology considered in this investigation are excellent materials for examining the effect of cell size on physical properties. This is due to the isotropic cellular structure, lack of residues of foaming agent, constant formulation, constant cell shape and ability to control and vary the cell size over a wide range.

Thermal conductivity depends on cell size, the magnitude of this dependence seems to change with density and it is greater for lower density foams. The property changes linearly with temperature, but the dependence on temperature in the black foam materials studied here is less than previously found for white LDPE foams. The conductivity variations with cell size can be predicted by a simple equation which takes into account the heat flow mechanisms through the foam. Black foams have shown a lower thermal conductivity than white foams of the same density and cell size.

Young's modulus, non-recoverable strain and collapse stress seem to be approximately constant as a function of cell size. However, the slope of the initial part of the compressive stress strain curve reduces with cell size between the 2^{nd} and 5^{th} loading cycles. Due to the relationships between the thermal expansion and Young's modulus these two properties follow the same trends as a function of cell size.

Although the mechanical properties at low strain rates and room temperature seem to be independent of cell size, the dynamic mechanical properties shows a dependence on it at temperatures below 15°C. This property is mainly affected by the morphology of the base polymer, therefore this result suggests a variation in polymer morphology with cell size, a conclusion that it is reinforced by the microstructural characterisation of the foams.

Finally, the study of polymer morphology and its representation in terms of functional relationships has been particularly difficult because of the modifying effect of the superimposed cellular structure. This is particularly noticeable when polyolefin foams are considered. It has been pointed out that cellular structure, initial formulation and polymer morphology are not independent variables. During the crystallisation of the foam there are interactions between these variables. This fact seems to have interesting effects on the final properties. This is an interesting research subject that, in our opinion, should be analysed in the future.

ACKNOWLEDGEMENTS

Financial assistance from the CICYT (MAT 99-0979) and from JCYL (VA67/00) is gratefully acknowledged. We also thank Zotefoams Plc. for supplying the foams.

REFERENCES

1. Rodees, M.B., "A Perspective on Cell Morpholohy and Foam Properties", in Polymeric Foams: Science and Tecnology, Ed., Khemani, K.C, ACS Symposium Series, American Chemical Society, (1997)
2. Glicksman, L.R., in "Low Density Cellular Plastics: Physical Basis of Behaviour", Hilyard, N.C., Cunningham A., (Ed.), Chapman and Hall, (1994)
3. Leach, A.G., *J. Phys. D: Appl. Phys.*, 26, (1993), 733
4. Colishaw, P.G., Evans, J.R.G., *J. Mater.Sci.*, 29, (1994), 486
5. Gibson, L.J. and Ashby, M.F. Cellular Solids: Structure and Properties, Pergamon Press, Oxford, England, (1988)
6. Hilyard, N.C., Cunningham A., in "Low Density Cellular Plastics: Physical Basis of Behaviour", Hilyard, N.C., Cunningham A., (Ed.), Chapman and Hall, (1994)
7. Brezny R.and Green D.J., Acta Metal Mater. 38 (12), (1990), 2517-2526
8. Almanza, O.A., Rodríguez-Pérez, M.A. and de Saja, *J.A. Cel. Polym.*, 18(6), (1999). 385
9. Almanza, O.A., Rodríguez-Pérez, M.A., de Saja, *J.A. J. Polym. Sci.: Polym. Phys.*, 38, (2000), 993-1004
10. ASTM D3576, Annual Book of ASTM Standards, Vol 8.02, (1994)
11. Kuhn, J., Ebert, H.P., Arduini-Schuster, M.C., Büttner, D. and Fricke J., *Int. J. Heat Mass Transfer*, 35, (1992), 1795
12. B. Wunderlich, in *"Macromolecular Physics"*, Vol 2, Academic Press, New York, (1973-1976)
13. A.Dobreva-Veleva and I. Gutzow, *J. Non. Cryst. Solids*, 162, (1993), 13-25
14. Shahin, M.M., Olley R.H., Blisset, M.J., *J. Polym. Sci.: Polym. Phys.*, 37, (1999), 2279

15. Rodríguez-Pérez, M.A., Alonso, O., Duijsens, A., De Saja, J.A., *J. Polym. Sci. Polym. Phys. Ed*., 36, (1998), 2587
16. Hilyard, N.C., in *"Low Density Cellular Plastics: Physical Basis of Behaviour"*, Hilyard, N.C., Cunningham, A., (Ed.), Chapman and Hall, London, (1994)
17. Rodríguez-Pérez, M.A., Rodríguez-Llorente, S., Saja de, J.A., *Polym. Eng. Sci.,*37, (1997) 959.
18. Mills, N.J., Gilchrist, A., *J. Cell.Plast*., 33, (1997), 1264
19. Almanza, O.A., Rodríguez-Pérez, M.A., de Saja, *J.A. Polymer*, 38, (2000), 993-1004
20. Martínez-Diez, J.A, Almanza, O., Arcos, L.O., Rodríguez-Pérez M.A., de Saja, J.A., *J. Cell. Plast*., 37, (2001), 21-42
21 Handbook of Chemistry and Physics, 53rd Ed., CRC Press
22. Mills, N,J., Gilchrist, A. *Cell. Polym*. 16, (1997), 87
23. Almanza O., Árcos y Rábago L.O., Rodríguez-Pérez M.A., de Saja J.A*., J. Macrom. Sci.:Phys*., B40(3&4), (2001), 603-613
24. Alberola, N., Cavaille J.Y., and Pérez J., *J. Polym. Sci. Polym. Phys*., (Ed.), 28, (1990), 569
25. Popli P., Glotin, M., Mandelkern. L, and Benson, R.S., *J. Polym. Sci. Polym. Phys. Ed*., 22, (1984), 407